Adsorption and Reaction of Small Molecules on Oxide Surfaces

H. Kuhlenbeck and H.-J. Freund

Lehrstuhl führ Physikalische Chemie I, Ruhr-Universität Bochum, Universitätsstraße 150, W-4630 Bochum, Germany

1. Introduction

Oxides are important materials in a variety of aspects. The most prominent field of application of oxides is catalysis, where oxides are employed both as active catalysts as well as supports [1-2]. Almost everything we know about adsorption and reaction of molecules on oxide surfaces we know from infrared studies on oxide powder surfaces [2]. However, it is our view [3-7] that these studies should be supplemented by investigations of single crystalline oxide surfaces in order to reveal information on the geometric and electronic structure of the adsorbed molecules as well as the influence of crystal orientation on adsorption. Several groups have started in recent years to study the adsorptive behaviour of bulk oxide single crystals [1,8,9]. If the oxide has low thermal and electric conductivity the established methods in surface science, which are often electron spectroscopic methods, cannot be used due to surface charging effects. A way out is to use epitaxially grown oxide films on metal substrates which do not show charging effects in those cases where oxide bulk single crystals are not suitable [3-7].

The present review first dicusses the methods that may be used to form epitaxial oxide films, and then presents some of our recent results on the study of adsorption of small molecules such as CO, CO_2 and NO on Cr_2O_3(111) [4,5,7], NiO(100) [3,10] and Al_2O_3(111) [6] surfaces.

2. Oxide film preparation

There are basically three techniques that have been applied in the past to form epitaxial oxide films. As shown schematically in Fig. 1a oxidation of a metal single crystal may be a reasonable route to achieve this goal. This works for example for Ni and Cr, and in the case of Ni one may even form oxide surfaces of different crystallographic orientations, i.e. (100) and (111). Note at this point that for fcc oxides the (111) surfaces are often so called polar surfaces which are characterized by divergent Madelung energies if no charge reorganisation occurs at the surface. If the film thickness remains low, however, the surface may be kept stable. In other words, investigation of thin films allows us to investigate crystallographic orientations of oxid surfaces which are unstable for bulk systems but are known to exist in powder samples. Another route is to evaporate a metal onto an inert metallic substrate possibly within an oxygen atmosphere and deposite in this fashion an oxide film (Fig. 1b). This method has been applied to NiO [3,10] and ZrO_2 [11] films. For example, NiO(100) grows on Ag(100) and Au(100) surfaces whereas NiO(111) grows on a Au(111) surface [12]. The third method that we would like to mention is the oxidation of alloy surfaces (Fig. 1c). One may either end up with ternary oxides or as in the case of NiAl(110) with an oxide surface of the metal with higher exothermicity, i.e. γ-Al_2O_3(111) [8].

Springer Proceedings in Physics, Vol. 73
Editors: R.F. Howe, R.N. Lamb, K. Wandelt

Fig. 1 Methods of thin oxide film preparation

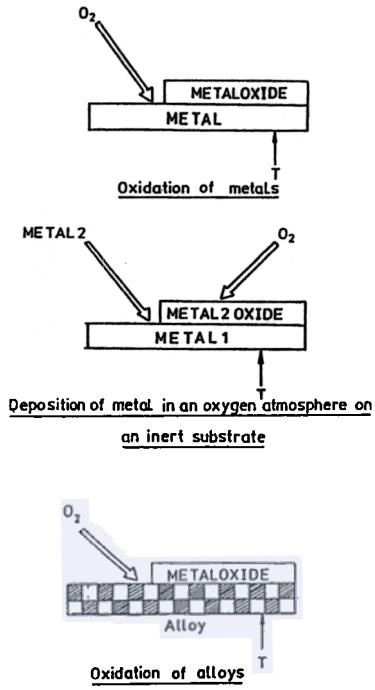

3. Adsorption on oxide surfaces

3.1 $Cr_2O_3(111)$

A particularly interesting oxide surface that has been investigated by several groups with respect to structure and vibrational properties in the past is the $Cr_2O_3(111)$ surface grown on top of a Cr(110) metal substrate [13-16]. A $Cr_2O_3(111)$ surface may be formed via direct oxidation of the metal substrate. The surface exhibits a hexagonal LEED pattern (Fig. 2a) if prepared in ultrahigh vacuum or via cleaving of a Cr single crystal in air. Recently it was shown that STM micrographs can be taken on a thin $Cr_2O_3(111)$ film (Fig. 2b) [17].
It appears thus that according to the high stability of the surface the chemistry of this surface is expected to be rather dull. However, the contrary is the case as we shall show in the following: When a $Cr_2O_3(111)$ surface is prepared in vacuo it exhibits an EL spectrum as shown in the bottom of Fig. 3. The losses, due to electronic excitations of the system, may be grouped into two regimes, i.e. the d-d transitions and the charge-transfer transitions. A loss at 1.2 eV is characteristic for the flashed surface and very sensitive to molecular dissociative adsorption when oxygen is involved. A detailed analysis shows that this loss indicates the presence of Cr^{2+} in the topmost layer of the clean surface which is oxidized to Cr^{3+} via oxygen dissociation [4,5,7].
The HREEL spectra of the oxygen covered surface (Fig. 4) proove the formation of a new species via an adsorption induced band at $1003cm^{-1}$. It is not unlikely that this band is due to Cr=O double bonds as judged by the similar vibrational frequency ($990cm^{-1}$, $1000cm^{-1}$) in CrO_2Cl_2 [18]. Once these Cr=O bonds are formed on the surface the

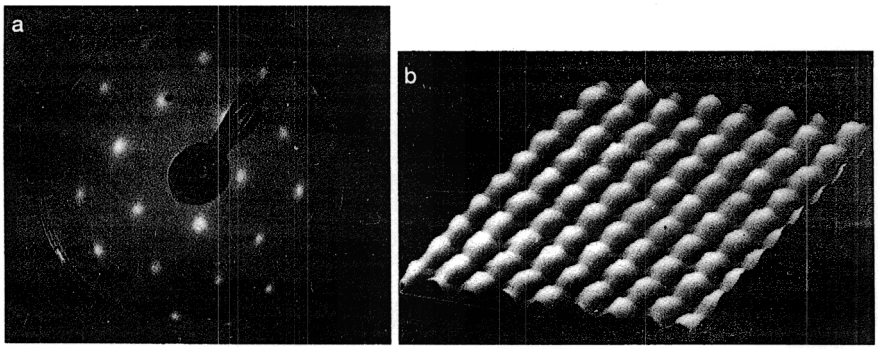

Fig. 2 a) LEED pattern of Cr_2O_3(111) surface prepared under UHV conditions on top of a Cr(110) surface b) STM picture of a native Cr_2O_3(111) surface prepared via cleavage of a Cr single crystal in air. [17]

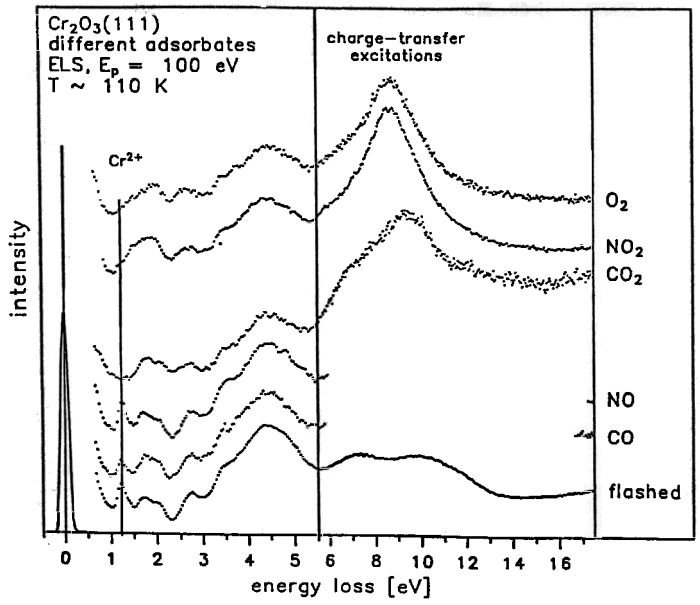

Fig. 3 Electronic excitations as measured via electron energy loss spectra of clean and adsorbate covered Cr_2O_3(111) surfaces

system is rather unreactive towards further adsorbates. However, not the whole Cr_2O_3(111) surface is covered with Cr^{2+} ions as may be suspected. ISS investigations [7] reveal that about half of the surface is covered with oxygen ions and the other half with Cr ions. Only the Cr terminated patches exhibit chemical reactivity in the sense discussed above.

If the flashed surface, i.e. the one exposing Cr terminated patches to the gas phase, is treated with CO_2 a carbonate forms already at low temperature as is indicated by ARUPS and HREELS [7]. Without going into the details of this aspect the carbonate is oriented perpendicular to the surface and bound to the surface in a bidentate configura-

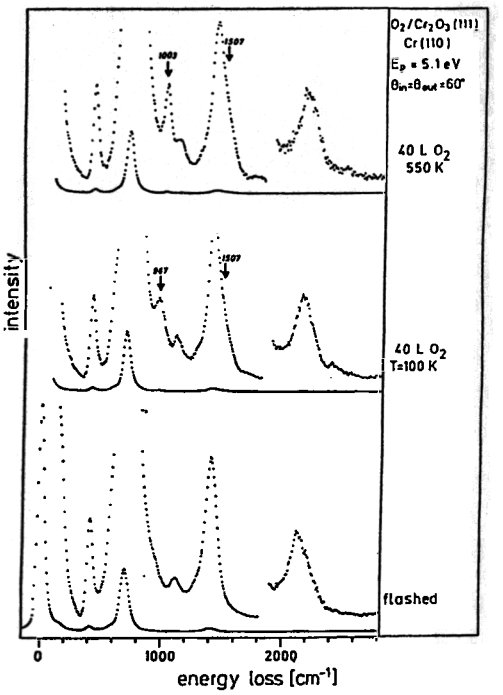

Fig. 4 Vibronic excitations as measured via electron energy loss spectra of clean and oxygen covered Cr_2O_3(111) surfaces

tion with two bonds towards different chromium ions [7]. Even though in this case dissociation of CO_2 into CO and O is only a minor reaction channel the Cr^{2+} ions are oxidized on the surface in the process of carbonate formation. Experiments involving isotopic labelling have to be performed in order to reveal further details of the reaction mechanism [7].

A relatively detailed picture of the adsorptive behaviour has been gained for CO adsorption. The ELS spectrum after CO adsorption still shows Cr^{2+} on the surface.

Fig. 5 shows photoelectron spectra of the $(\sqrt{3}x\sqrt{3})R30^o$ CO structure recorded in the so called forbidden and allowed geometries [19,20] as indicated in the figure in comparison with a normal emission spectrum of a physisorbed monolayer CO on Ag(111) [21].

There are two CO induced features visible in the spectra of the CO adsorbate on Cr_2O_3(111); one at 17.5 eV and a slightly asymmetric one at 20.2 eV. The CO σ valence emission should be intense at the photon energy the spectra have been taken with, i.e. 36 eV, whereas the 1π emission should be rather weak. Thus we identify the two CO induced features as the σ-ion states of molecularly adsorbed CO.

The electronic binding energies of CO on Cr_2O_3(111) are larger by several eV compared to those of the CO physisorbate on Ag(111). This holds also for CO adsorbates on other metals (see for instance refs. [21-23]), indicating that the substrate-CO interaction on Cr_2O_3(111) is appreciably different from that on metals.

Obviously, there is no significant difference in the spectra of CO/Cr_2O_3(111) for the two collection geometries in Fig. 5. If the CO molecular axis were oriented perpendicular to the surface, the symmetry selection rules would require the σ ion states to disappear in the forbidden geometry, and only the ion states of π-symmetry should show up. Since both σ-ion states of CO are observed with comparable intensities in both geometries, we conclude that the CO axis is strongly inclined with respect to the surface normal.

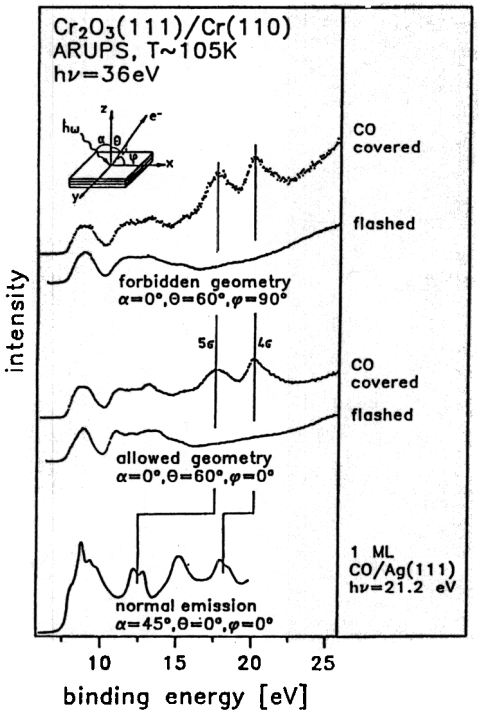

Fig. 5
Photoelectron spectra of CO($\sqrt{3} \times \sqrt{3}$)R30°/Cr_2O_3(111) taken in the allowed and forbidden geometries in comparison with the system CO/Ag(111)

More detailed information on the orientation of the molecular axis can be deduced from Fig. 6, where a set of photoelectron spectra taken with a constant angle, i.e. 90°, between the directions of light incidence and electron detection is shown.

From Fig. 6 it is obvious that the σ-ion states exhibit highest intensities for near normal light incidence and near grazing electron emission whereas at grazing light incidence these features are strongly attenuated, in strong contrast to CO adsorbed standing up on most metal surfaces. Since at a photon energy of 36 eV the σ states emit with highest intensity if the polarization direction and the direction of electron detection both coincide with the CO molecular axis this behaviour is only compatible with an orientation of the molecular axis approximately parallel to the surface.

In the inset of Fig. 6 we compare the emission intensities of the CO σ valence states as a function of photon energy for two different experimental geometries. The data shown in the upper panel were taken at a light incidence angle of 20° with respect to the surface normal, collecting the electrons 70° off normal whereas the data in the lower panel were taken at normal electron emission and near grazing light incidence (α = 80°). Obviously a strong σ shape resonance is observed only for grazing electron detection, again clearly indicating that the CO molecules must be strongly tilted.

The same conclusion about the molecular geometry must be drawn from the analysis of our NEXAFS (Near Edge X-ray Absorption Fine Structure) data [7]. These data show that the intensity of the π resonance varies only slightly as a function of the light incidence angle as expected for CO molecules lying flat on the surface since one 2π component is oriented parallel to the surface whereas the other one sticks out of the surface. A quantitative estimation of the tilting angle was not possible from our NEXAFS data since the σ resonance was so weak that its intensity only could be evaluated with very large error bars.

From the data discussed so far a quantitative evaluation of the tilting angle was not possible but tentatively we estimate this angle to be larger than about 70°.

An open question is: where are the 1π orbitals. For flat lying CO molecules the 1π levels are expected to split into two components, $1\pi_{xy}$ and $1\pi_{z^2}$ the first one oriented pa-

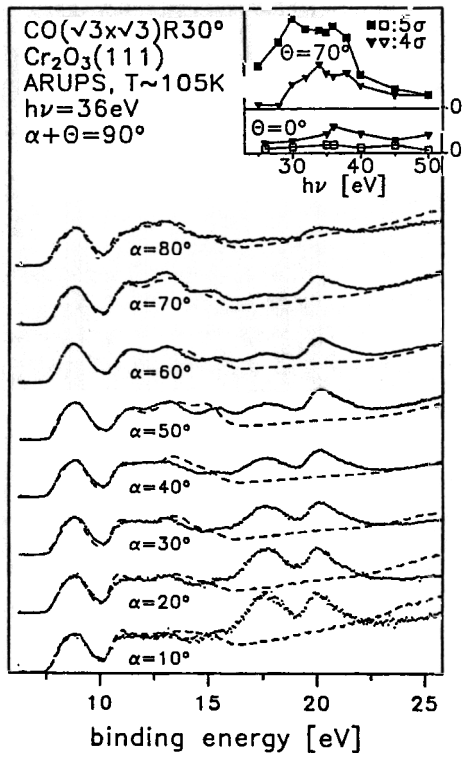

Fig. 6
Photoelectron spectra at various detection geometries. The inset shows the variation of the peak intensities with photon energy.

rallel to the surface and the other one oriented perpendicular to the surface. Whereas the $1\pi_{xy}$ emission might be hidden below the σ emissions because this level should be intense at grazing emission angles like the σ orbitals, the $1\pi_z$ should be intense at normal emission where the σ emission is weak. As can be seen from Fig. 6 the 5σ emission is nearly totally suppressed at near normal electron emission so that the $1\pi_z$ level is most likely not situated near to the 5σ level as is the case for the 1π levels of CO adsorbed on most metals. One might suppose that the $1\pi_z$ level is located somewhere in the region of the substrate bands but since the $1\pi_z$ orbital will interact strongly with the these bands it will most likely be shifted to higher binding energy because the substrate levels are energetically located above the 1π levels. Considering this it seems to be rather unlikely that the 1π levels are located somewhere in the region of the oxide emission.

Whereas the 5σ emission is nearly totally supressed at near normal emission a broad feature remains in the region of the 4σ between 19 and 22 eV (Fig. 6). Since the 4σ and the 5σ emission intensity should behave similar, it is tempting to attribute the remaining emission between 19 eV and 22 eV to the $1\pi_z$ level. Another possible assignment would be that this feature is due to a σ shake up state. However, we consider this to be unlikely because such shake up states should be intense at emission angles where the σ main lines are also intense, which is not the case.

Fig. 7 compares the binding energies of the present spectra with data reported in the literature [21-26]. All binding energies are larger than the corresponding values known from metal surfaces. They are even larger than the gas phase values. This holds also for the C1s ionization which is found 0.7 eV below its gas phase value [11]. The most interesting finding, however, is the energetic position of the $1\pi_z$ level which is in the present case most likely situated near to the 4σ level, indicating a fundamentally different interaction of the molecule with the surface as compared with all cases observed so far: The CO lone pairs (4σ and 5σ) we propose to be bound towards two different Cr ions in the sense of two σ-donor bonds which shift the σ binding energies to higher

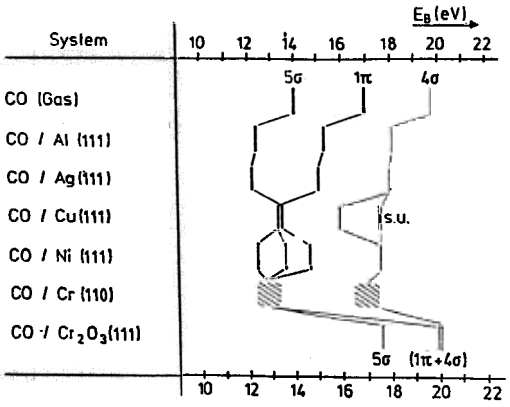

Fig. 7
Comparison of binding energies with respect to the vacuum level for various CO adsorbates and free CO. [5]

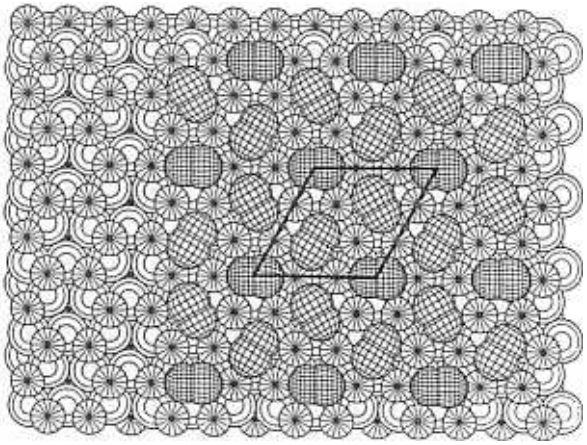

Fig. 8 Schematic representation of a $(\sqrt{3} \times \sqrt{3})R30°$ $CO/Cr_2O_3(111)$ structure as deduced from the combination of experimental evidences.

values. If this is true then it is very reasonable to assume that the 1π levels interact with both the Cr ions but in addition, and more importantly, with the oxygen layer underneath the terminating Cr layer. This latter interaction between the closed shell O^{2-} ions and CO must be basically repulsive. Since the oxygen levels are situated at lower binding energies than the CO 1π levels, the $1\pi_z$, which is the one that strongly interacts with the O^{2-} ions, is shifted towards higher binding energy and the interacting O^{2-} levels are rearranged as well. The shift of the $1\pi_z$ level is recognized in the data, while it is more difficult to identify the effect onto the oxygen levels. If we judge the observed shifts of CO on $Cr_2O_3(111)$ with respect to gaseous CO we find a shift of all CO levels to higher binding energies. The shift of the 5σ level is larger than the one of the 4σ level. This is very reasonable because it follows the individual polarizabilities of the levels involved. The interaction may be separated into the two bonding Cr-CO(5σ) and Cr-OC(4σ) interactions, and into a repulsive O^{2-}-CO(1π) interaction, leading to a weakly chemisorptive CO-Cr_2O_3 bond. The bonding of CO towards $Cr_2O_3(111)$ is completely different from the bonding of CO to a metallic Cr surface. It is a pure accident that CO binds to metallic Cr in a flat bonding geometry as well. The ion state binding energies as well as their sequence are clearly different from the situation on $Cr_2O_3(111)$ as may be seen from the data collected in Fig. 7.

A structure model of CO on the Cr-terminated patches of $Cr_2O_3(111)$ is presented in Fig. 8 where we show a schematic representation of the CO covered surface. The

($\sqrt{3}$x$\sqrt{3}$)R30° unit mesh is indicated. As suggested by the intensity of the CO valence band emission the surface is most likely rather densely covered with CO molecules as is for instance the case for CO on Ag(111) or N_2 on graphite [22] where the molecules are also lying flat on the surface. A structure with one molecule per unit cell would contain only the molecules on the corners of the ($\sqrt{3}$x$\sqrt{3}$) R30° unit mesh. In case the unit cell contains more than one molecule the other molecules have to be added.

The ordered structure is a clear indication that the adsorbate site cannot be a defect site. We find this confirmed also for an other adsorbate system on an oxide surface, i.e. NO on nonpolar oxide surfaces such as the NiO(100) surface.

3.2 NiO(100)

3.2.1 Geometric and electronic structure

We have investigated the adsorption of NO on a thin NiO(100) film of several layers thickness grown on top of a Ni(100) surface in comparison with data of an *in vacuo* cleaved NiO(100) single crystal [3]. The layer exhibits a high defect density. We demonstrate via application of several surface-sensitive electron-spectroscopic techniques (XPS, ARUPS, NEXAFS, HREELS) that the occupied (ARUPS) and unoccupied (NEXAFS) electronic states are similar to those of a bulk NiO(100) sample. In spite of its limited thickness, the band structure of the thin film exhibits band dispersions perpendicular to the surface that are compatible with those of bulk NiO(100). It is shown that the electronic structure of the oxygen sublattice can be described in a band-structure picture while for the Ni sublattice electron localization effects lead to a breakdown of the band-structure picture.

NO on NiO desorbs at 220 K. Fig. 9 shows the thermal desorption spectra of NO from a bulk Ni(100) surface in comparison with desorption from the oxide layer [3]. The desorption temperatures for both systems are only marginally different. If we consider the different heating rates and identical, commonly used frequency factors we calculate on the basis of the Redhead formula [27] almost identical desorption energies for both cases, i.e., 0.52 eV. This means that NO is weakly chemisorbed on a NiO surface. It is quite surprising that the desorption energies on both surfaces are the same because the defect densities are different by orders of magnitude as judged from the LEED spots [10], and one is tempted to expect a strong influence of the defects on the desorption temperature. However, even though we do not know the exact nature of the defects the

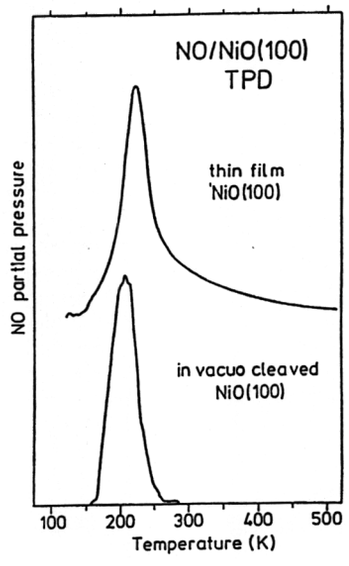

Fig. 9 Thermal desorption spectra of NO desorbing from the NiO(100) surfaces of a thin film and a bulk crystal.

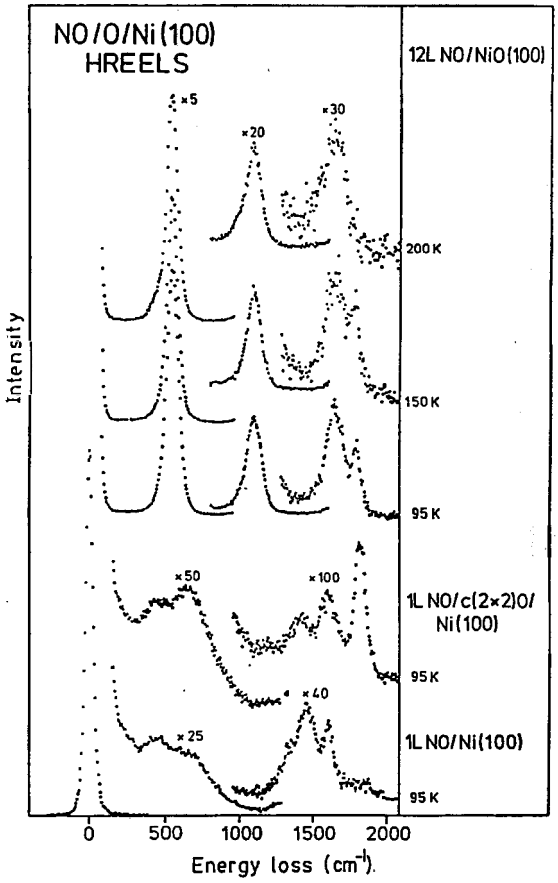

Fig. 10
Vibronic excitation as measured via electron energy loss spectra of a clean and a NO covered NiO(100) surface in comparison with spectra of NO and an NO + O coadsorbate on Ni(100)

similarity of the desorption temperatures indicates that the defects are not the sites of NO adsorption on the oxide film. The NO coverage is close to 0.2 relative to the number of Ni surface atoms as determined by XPS. HREELS reveals that there is only one species on the surface documented by the observation of only one bond-stretching frequency.

Fig. 10 shows some HREEL spectra of NO on a NiO(100) film at different temperatures. Upon exposure to NO at low temperature, we observe in addition to the very strong NiO surface phonons one peak at the high-frequency side of the third multiple-phonon-loss. This peak vanishes at about 200 K surface temperature in agreement with the thermal desorption data which showed a peak temperature only a little above T = 200 K. We assign this peak to the N=O bond-stretching vibration of NO adsorbed on top of Ni sites in the NiO layer. This assignment is based on a detailed HREELS study of NO-O-coadsorption on Ni(100) [28]. We have plotted HREELS spectra of NO on Ni(100) and NO + O on Ni(100) for comparison in Fig. 10. Both spectra are rather complex, and a detailed discussion shows that the spectra are caused by the superposition of a set of different species [28]. The important aspect for the present purpose is the appearance of a single peak at 1800 cm^{-1} for adsorption near coadsorbed oxygen. This peak has been assigned to NO adsorbed on top of Ni atoms with a bent Ni-NO bond. The bending of the axis in the coadsorbate is also indicated by the appearance of a bending vibration at 640 cm^{-1}, typical for a strongly bound system [29].

We have transferred this assignment to the oxide surface although we do not observe a bending mode. We cannot exclude at present that such a bending vibration is si-

tuated near the position of the NiO phonon loss but this would imply that the force constant of the bending mode on the oxide surface is similar to the adsorbate on the metal surface. However, we know that the molecule-substrate-bonding is much weaker on the oxide surface as compared with the metal surface, so that we expect a reduced bending force constant. This would shift the bending mode to lower frequencies which might render the bending mode unobservable under the present conditions. Clearly, an independent experimental clue as to the geometry of the molecular axis is highly desirable. We have therefore performed NEXAFS investigations on the NO/NiO(100) adsorbate [3]. NEXAFS data on the system and a comparison with previous data on the system NO/Ni(100) indicate that the molecular axis of adsorbed NO is tilted by an angle of approximately 45° relative to the surface normal. The N1s XP spectra of the weakly chemisorbed species show giant satellites similar to the previously observed cases for weak chemisorption on metal surfaces. This is the first observation of an intense satellite structure for an adsorbate on an insulator surface, which shows that there must be sufficient screening channels even on an insulating surface. A theoretical assignment of the peaks has been discussed [3]. We compare the spectroscopic properties of the NO species on the thin-film oxide surface, which is likely to contain a certain number of defects, with NO adsorbed on a basically defect-free bulk oxide surface by TD and XP spectra. TD and XP spectra of the bulk system are basically identical as compared with the oxide film, indicating that the majority of species adsorbed on the films is not adsorbed on defects but rather on regular NiO sites. Results of *ab-initio*-oxide-cluster-calculations are used to explain the bonding geometry of NO on regular NiO sites [3].

3.2.2 Desorption dynamics

Oxide surfaces are ideally suited to study photochemical desorption reactions. This is due to existence of a band gap at the Fermi energy and the high degree of localization of the electronic charge in these ionic systems. Both characteristics lead to a situation where the excitation energy pumped into the adsorbate stays on the adsorbate long enough to allow for desorption with very high yields [30-34]. In particular this is in contrast with adsorbates on metal surfaces where the excitation is dissipated into the substrate very fast via low energy electron-hole pair creation for example so that desorption is quenched very efficiently. The high yields in the case of oxide surfaces allow us to measure the distribution of energy into the internal degrees of freedom as well as into the translational energy of the desorbing particles. For these measurements we use a setup scetched in Fig. 11 [34].
Desorption is stimulated via an ArF-eximer laser with 193nm wave length (ca. $2 mJcm^{-2}$; pulse duration 20-25ns) at normal incidence to the surface. The details of the experimental setup are discussed elsewhere. Briefly, the desorbing particles are detected within a volume created by the beam of an excimer pumped dye laser oriented parallel to the surface plane. The molecules within this volume are excited, and the ions are repelled into a drift tube and finally detected via a set of multichannel plates and a phosphorous screen. The two dimensional image can be stored via a computer controlled CCD-camera. Fig. 12 shows several velocity distributions measured for different quantum numbers N of the angular momentum of the NO molecules desorbing from a NiO(100) surface. The important message of Fig. 12 is: There are two maxima in the velocity distribution which show different dependences on the variation of angular momentum: The position of the maximum at lower velocity is independent of the rotational quantum number N while the position of the maximum at higher velocities moves to higher velocities for larger rotational quanta. Very similar bimodal velocity distributions were obtained for all three lowest vibrational quanta (v = 0,1,2).

Fig. 12 shows for one rotational state, i.e. N = 10, the velocity distributions for the three lowest vibrational states. From the population of the vibrational quanta a vibrational temperature may be estimated as $T_v = 1890 \pm 50$ K, being far above the surface temperature of $T_s = 90$ K. From Boltzmann plots we deduce rotational temperatures of $T_R = 260$ K and 470 K for the fast channel and $T_R = 410$ K for the slow channel, independent of the vibrational state. Earlier we had assumed that the "fast" channel is due to non-thermal and the "slow" channel due to thermally equilibrated desorption processes. However, our present results indicate that both channels represent non-thermal processes. The desorption cross section for NO from NiO(100) is of the order of 10^{-17} cm^2

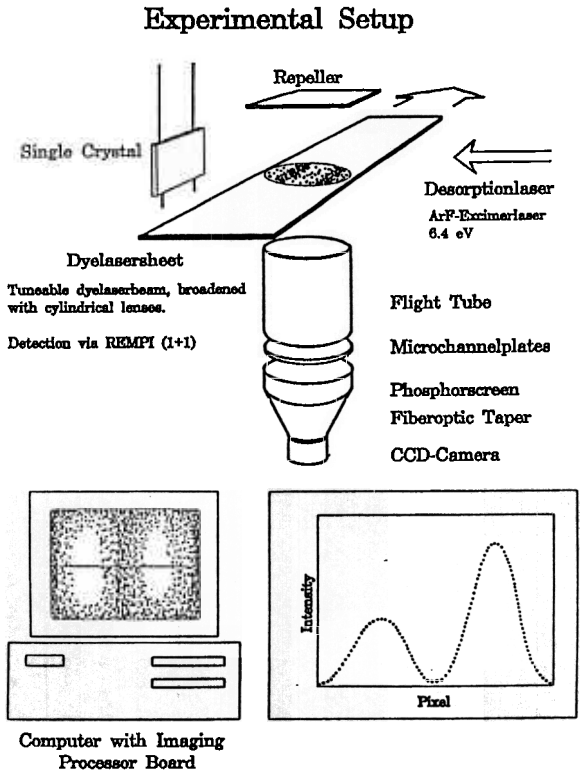

Fig. 11 Schematic representation of the experimental setup to study laser induced desorption

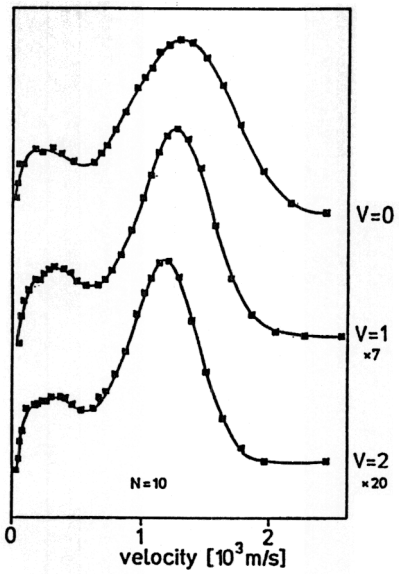

Fig. 12
Velocity distributions of NO molecules desorbing from NiO(100) after laser excitation for three different vibrational (v = 0,1,2) and the same rotational state (N = 10)

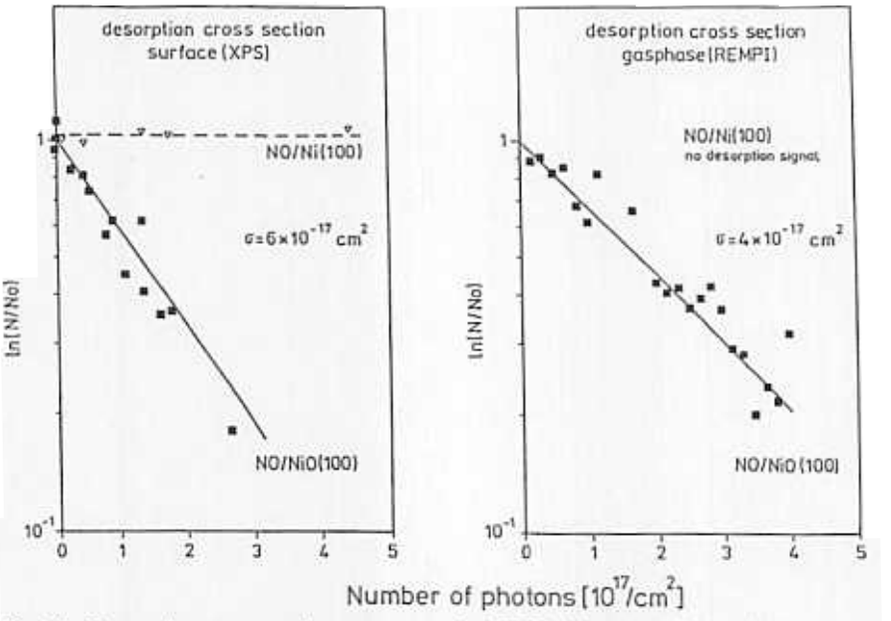

Fig. 13 Desorption cross-section as measured via XPS (a) on the NiO(100) surface and via REMPI (b) in the gas phase

as determined by measuring both the number of NO molecules remaining on the surface as well as those desorbing into the gas phase as shown in Fig. 13 where in a half logarithmic plot the surface (Fig. 13a) respectively gas phase (Fig. 13b) concentrations are plotted versus the number of photons. This cross section is at least four orders of magnitude larger as compared with NO on a Ni(100) metal surface where we could not detect desorption within the limits of our experimental setup.

We have carried out trajectory calculations [34] to simulate the desorption processes, and these calculations allow us to suggest an explanation for the existence of bimodal velocity distributions: In a classical picture the two maxima are connected with the instant at which the molecule surface bond of the system vibrating with respect to the surface is ruptured. The maximum at high velocities is assigned to molecules moving away from the surface when the electronic excitation occurs, the maximum at low velocities is due to molecules excited on the way towards the surface. The velocity difference between the two maxima depends on the life time of the molecule in the excited state.

The observed vibrational populations of the desorbing molecules are described by model calculations assuming the intermediate formation of a negative NO ion. The longer N-O equilibrium bond length in NO^- as compared to neutral NO in the ground state is responsible for the vibrational excitation in our model. We estimate relaxation times for the vibrational processes which are compatible with a rotational-translational relaxation time of $4 * 10^{-14}$ sec.

3.3 Al_2O_3(111)

As the last example we would like to discuss the case of Al_2O_3 [6]. Aluminiumoxide is the prototype of a support material and particularly interesting in this respect. An Al_2O_3 layer with a quasihexagonal oxygen layer as the terminating surface may be grown via oxidation on top of a NiAl(110) alloy surface. The oxide layer is very thin, i.e. it exhibits a thickness of about 5 Å. The oxygen-oxygen distance in the quasihexagonal oxygen layer

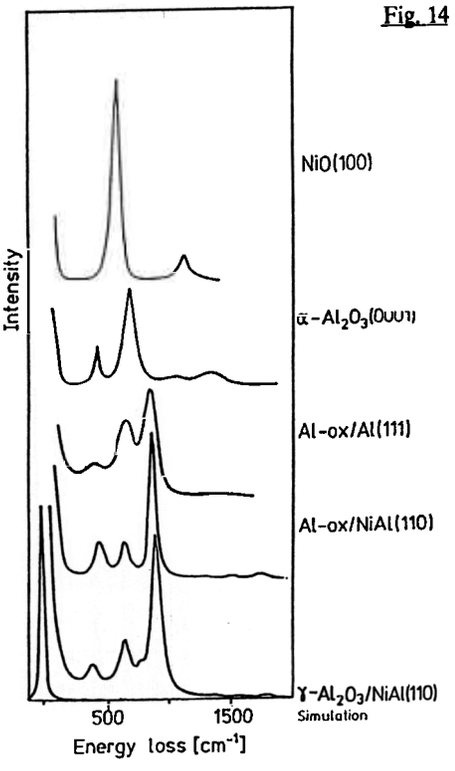

Fig. 14 Vibronic excitation as measured via electron energy loss spectra of Al_2O_3(111) on NiAl(110) in comparison with HREELS spectra from various substrates.

is by about 6% larger as compared with bulk Al_2O_3 but this is compatible with the limited thickness of the film. We believe from our HREELS data that this oxide film is related to a (111) γ-Al_2O_3 surface as revealed by Fig. 14. In this figure a comparison of HREEL spectra of different substrates is shown. While the spectrum of the thin film does not correlate with NiO nor with α-Al_2O_3 it is similar to a thin Al_2O_3 layer grown on top of a Al single crystal surface. At the bottom a spectrum calculated for γ-Al_2O_3 is shown and compared with the data. The similarity is striking and becomes even better if we take into account that the film from which the spectrum was recorded has been prepared by using ^{18}O. Therefore our conclusion so far is that by oxidation we grow a γ-Al_2O_3(111) like surface on top of the NiAl(110) alloy surface. It will be the next step to deposite metal clusters onto such a surface in order to possibly create well defined models for supported catalysts.

4. Synopsis

Adsorption of small molecules on well characterized oxide surfaces leads to new and unexpected adsorbate geometries with unusual electronic structures. Polar oxide surfaces as opposed to non-polar surfaces appear to be particularly active in this respect.

We have presented some examples of adsorption and reaction of small molecules like CO, CO_2 and NO on polar and non-polar surfaces.

These surfaces may be chemically reactive or rather inert, depending on the nature of the metal ions involved and on their tendency to form several oxidation states on the surface.

It has been pointed out that oxide surfaces are well suited substrates to investigate photochemically induced desorption processes. It is possible to determine experimen-

tally the distribution of the excitation energy into the internal and translational degrees of freedom of the desorbing particle. Via model calculations conclusions on the microscopic processes involved in the desorption mechanism may be drawn.

Acknowledgements

We would like to thank the Deutsche Forschungsgemeinschaft and the Ministerium für Wissenschaft und Forschung des Landes Nordrhein-Westfalen for financial support. H.-J. Freund is grateful to the Fonds der Chemischen Industrie.

References:

[1] H.H. Kung, "Transition Metal Oxides: Surface Chemistry and Catalysis", Elsevier Publishing Company, Amsterdam 1989.
[2] A.A. Davydov,"Infrared Spectroscopy of Adsorbed Species on the Surface of Transition Metal Oxides", John Wiley & Sons, Chichester, England (1980).
[3] H. Kuhlenbeck, G. Odörfer, R. Jaeger, G. Illing,M. Menges, Th. Mull, H.-J. Freund, M. Pöhlchen, V. Staemmler, S. Witzel, C. Scharfschwerdt, K. Wennemann, T. Liedke and M. Neumann, Phys. Rev. B 43, 1969 (1991).
[4] C. Xu, M. Hassel, H. Kuhlenbeck, H.-J. Freund, Surf. Sci. 258, 23 (1991)
[5] C. Xu, B. Dillmann, H. Kuhlenbeck, H.-J. Freund, Phys. Rev. Lett. 67, 3551 (1991)
[6] R.M. Jaeger, H. Kuhlenbeck, H.-J. Freund, M. Wuttig, W. Hoffmann, R. Franchy, H. Ibach, Surf. Sci. 259, 235 (1991)
[7] H. Kuhlenbeck, C. Xu, B. Dillmann, M. Haßel, B. Adam, D. Ehrlich, S. Wohlrab, H.-J. Freund, U.A. Ditzinger, H. Neddermeyer, M. Neuber, M. Neumann, Ber. Bunsenges. Phys. Chem., 96, 15 (1992)
[8] V.E. Henrich, Rep. Prog. Phys. 48, 1481 (1985)
[9] "Surface and Near Surface Chemistry of Oxide Materials" (Eds. J. Nowotny, L.-C. Dufour) Material Sci. Monogr. Vol 47, Elsevier (1988)
[10] M. Bäumer, D. Cappus, H. Kuhlenbeck, H.-J. Freund, G. Wilhelmi, A. Brodde, H. Neddermeyer, Surf. Sci. 253, 116, (1991)
[11] V. Manrice, M. Salmeron, G.A. Somorjai, Surf. Sci. 237, 116 (1991).
[12] H. Neddermeyer, private communication
[13] P. Michel and C. Jardin, Surf. Sci. 36, 478 (1973)
[14] S. Ekelund and C. Leygraf, Surf. Sci. 40, 79 (1973)
[15] F. Watari and J.M. Cowley, Surf. Sci. 105, 240 (1981)
[16] H.M. Kennett and A.E. Lee, Surf. Sci. 33, 377 (1972)
[17] N.M.D. Brown, H.-X. You, Surf-Sci. 253, 317 (1990)
[18] F.A. Miller, G.L. Carlson, W.B. White, Spectrochim. Acta 15, 709 (1959)
W.E. Hobbs, J. Chem. Phys. 28, 1220 (1958)
[19] E.W. Plummer and W. Eberhardt, Adv. Chem. Phys. 49, 533 (1982)
[20] H.-J. Freund and M. Neumann, Appl. Phys. A 47, 3 (1988)
[21] D. Schmeisser, F. Greuter, E.W. Plummer, and H.-J. Freund, Phys. Rev. Lett. 54, 2095 (1985)
[22] C. Jacobi, C. Astaldi, P. Geng, and M. Bertolo, Surf. Sci. 223, 569 (1989)
[23] H.-J. Freund, W. Eberhardt, D. Heskett, and E.W. Plummer, Phys. Rev. Lett. 50, 768 (1983)
[24] C. Schneider, H.-P. Steinrück, P. Heimann, T. Pache, M. Glanz, K. Eberle, E. Umbach, and D. Menzel, BESSY Annual Report, 1987 (unpublished)
[25] D.W. Turner, C. Baker, A.D. Baker, and C.R. Brundle, Molecular Photoelectron Spectroscopy (Wiley-Interscience, New York, 1970)
[26] N.D. Shinn, J.Vac.Sci.Technol. A 41, 1351 (1986)
[27] P.A. Readhad, Vacuum 12, 203 (1962)
[28] G. Odörfer, R. Jaeger, G. Illing, H. Kuhlenbeck, H.-J. Freund, Surf. Sci. (1990)
[29] L.H. Jones, R.R.

[30] D. Weide, P. Andresen, H.-J. Freund, Chem. Phys. Lett. 136, 106 (1987)
[31] F. Budde, A.V. Hamza, P.M. Ferm, G. Ertl, D. Weide, P. Andresen, H.-J. Freund Phys.Rev.Lett., 60, 1518 (1988)
[32] P.M. Ferm, F. Budde, A.V. Hamza, S. Jakubith, G. Ertl, D. Weide, P. Andresen, H.-J. Freund, Surf. Sci. 218, 467 (1989)
[33] Th. Mull, M. Menges, B. Baumeister, G. Odörfer, H. Geisler, G. Illing, R.M. Jaeger, H. Kuhlenbeck, H.-J. Freund, D. Weide, U. Schüller, P. Andresen, F. Budde, P. Ferm, V. Hamza, G. Ertl, Physica Scripta, 41, 134 (1990)
[34] Th. Mull, B. Baumeister, M. Menges, H.-J. Freund, D. Weide, C. Fischer, P. Andresen, J.Chem. Phys., in press